Astron. Astrophys. 345, 1011–1018 (1999)

ASTRONOMY AND ASTROPHYSICS

Dynamics of solar active region loops

L.K. Harra-Murnion[1], **S.A. Matthews**[1], **H. Hara**[2], **and K. Ichimoto**[2]

[1] Mullard Space Science Laboratory, University College London, Holmbury St. Mary, Dorking, Surrey RH5 6NT, UK (lkhm, sam@mssl.ucl.ac.uk)

[2] National Astronomical Observatory, Mitaka, Tokyo 181, Japan (hara, ichimoto@solar.mtk.nao.ac.jp)

Received 18 November 1998 / Accepted 1 March 1999

Abstract. It has been frequently observed that in solar active regions the measured line widths are larger than those based on thermal equilibrium widths. This excess width (characterised as non-thermal velocity, V_{nt}) has been proposed as a signature of the heating mechanism. The behaviour of the V_{nt} at coronal temperatures has not produced consistent results with values ranging from 0 to 100 km s^{-1}. We investigate this problem by using joint observations from Norikura Solar Observatory, Japan and the Coronal Diagnostic Spectrometer (CDS) on SOHO. With CDS we determine temperatures, and with Norikura we obtain accurate line widths for Fe XIV (≈2 MK). We find that values of V_{nt} range between 10–20 km s^{-1}. We analyse the dynamical behaviour of different temperature loops and find that for loops with Log $T_e < 5.8$, the variability $\propto T_e^{0.39}$. This is comparable to the dependence of non-thermal velocity on temperature which we have determined to be $V_{nt} \propto T_e^{0.35}$. This suggests that the excess line broadening is caused by highly dynamical behaviour in the transition region for active regions. These results have significant implications for potential heating mechanisms and these are discussed.

Key words: Sun: corona – Sun: transition region – Sun: UV radiation – Sun: X-rays, gamma rays

1. Introduction

It is well observed that in flaring and non-flaring active regions the line widths are found to be in excess of the thermal width. This excess width has been termed *non-thermal velocity* (V_{nt}) and it is thought to be an indicator of the coronal heating mechanism. Transition region observations in both active regions and the quiet Sun (e.g. Boland et al. 1975, Doschek et al. 1976 and Mariska et al. 1978) show that the non-thermal velocity (V_{nt}) increases with increasing temperature ($V_{nt} \propto T_e^{1/4}$ for log $T_e < 5.8$). This behaviour is predicted from an Alfvén or acoustic wave propagating without energy dissipation. Similar behaviour of V_{nt} with temperature has also been seen in stars with hot coronae, as observed with IUE (Jordan 1991). Dere & Mason (1993) also observed that the active regions have higher values of non-thermal velocity than the quiet Sun.

However as coronal temperatures are reached the relationship becomes less clear. For coronal active region observations a range of results have been published; Tsubaki (1975) found values of V_{nt} to range between 6–16 km s^{-1} using the Fe XV/Fe XIV temperature diagnostic giving a temperature of 2.6 MK; Acton et al. (1981) found values of 100±28 km s^{-1} using the Ne IX/Mg XI temperature diagnostic which gives 4MK; Saba & Strong (1991) found values of 40–60 km s^{-1} using the O VIII, Ne IX, and Mg XI lines to give a temperature of 3MK; Sterling (1997) found values of on average 45 km s^{-1} using the ratio of satellite line to the resonance line of S XV as a temperature diagnostic giving values of between 5.5–6.2MK; Hara (1996) found magnitudes of 11–19 km s^{-1} by assuming the peak of the G(T_e) function for Fe X, Fe XIV and Ca XV to be 1MK, 1.8MK and 3.5 MK respectively. These examples show the wide ranging values of V_{nt} (10–100 km s^{-1}) which have been derived for temperatures ranging between 1–6.2MK. Although the dependence of V_{nt} with temperature below log T_e=5.8 has been verified, the behaviour above log T_e >5.8 is still not well understood. One of the assumptions that is generally made in the case of active regions is to assume that there is no temperature gradient and the active region is isothermal.

Another possibility to explain the excess line broadening is that there are multi-directional Doppler flows which could be a result of the superposition of flows in many magnetic flux tubes which are not spatially resolved. In active regions it has been found that cool transition region loops coexist with hot coronal loops (e.g. Orall 1981). Consequently there has been much recent support for the Unresolved Fine Structure (UFS) explanation of the transition region suggested by Feldman (1983). In this work Feldman suggests that the bulk of the transition region emission comes from a completely different entity to the traditional interface between chromospheric and coronal temperatures. Whilst the UFS are suggested to be low-lying cool loops, results from SOHO tend to lend support to the idea of transition region emission as a separate entity from chromospheric and coronal emission with large complete transition region temperature loops being observed at the same altitudes as the coronal loops (see also Fludra et al., 1997). The cool loops are not formed from the cooling down of hot loops (Matthews &

Send offprint requests to: L.K. Harra-Murnion

Harra-Murnion 1997). These various observations dictate that caution has to be used in assuming a link between the transition region emission and its relation to the coronal emission.

Different temperature loops in active regions have been found to show very different characteristics. The transition region cool loops ($<$ 1MK) are in general more dynamic than the hotter loops ($>$ 1MK). Sheeley (1980) discovered from Skylab data that the Ne VII structures (0.5 MK) had a lifetime on the order of 30 mins while the hotter Mg IX and Fe XV loops had lifetimes of 1.5 hrs and 6 days respectively. More recently, SOHO results have shown that the transition region temperature structures have large Doppler shifts in the range $\pm$ 50–100 km s^{-1} (Brekke, Kjeldseth-Moe & Harrison 1997). Kjeldseth-Moe & Brekke (1998) have analysed several datasets from CDS to look in particular for time variability and flows in active region loops. They found very dynamic behaviour with changes on time scales of 10–20 mins, for active region loops with temperatures in the 1–5 $\times$ 10^5 K range. Yoshida & Tsuneta (1996), have analysed temperature maps of coronal emission in active regions using the Yohkoh soft X-ray telescope. They found that loop structures with the highest temperatures (5–8MK) have the shortest lifetimes (few hours), whereas the lower temperature structures (3–4MK) have longer lifetimes. The difference in lifetimes suggests that the higher temperature (5–8MK) plasma is being heated transiently (e.g. by magnetic reconnection events) and the lower temperature loops (3–4 MK) are being heated in a more uniform manner. Observations covering a wide range of temperatures from the transition region to the corona have shown that different temperature loop structures can have different properties. If this is the case then the dependence of V_{nt} with temperature in active regions may be due to the different classes of loops which exist, and cannot be due to a wave which travels through the different temperature layers.

In this paper, we determine the values of V_{nt} in an active region without assuming that the region is isothermal in the radial direction. This is achieved by making use of the temperature diagnostic and spatial information available from the Coronal Diagnostic Spectrometer (CDS), and the measurements of the line widths from the Norikura Solar Observatory. Since a wide range of values have been determined for V_{nt} it is important to check the assumptions made in the determination of V_{nt}. This will have implications for the heating mechanism. Does the dependence of V_{nt} with temperature continue beyond log T_e=5.8?

The dependence of V_{nt} with temperature up to log T_e=5.8 in both the quiet Sun and active regions is reasonably well established. However, although the transition region emission in active regions is frequently in the form of highly dynamical loops, no consideration has been taken of this in terms of explaining the observed values of V_{nt}. We investigate the behaviour of different temperatures loops and relate this to the dependence of V_{nt} with temperature.

Sect. 2 briefly describes the instrumentation used and the observation mode. Sect. 3 gives an account of the determination of V_{nt} for coronal temperatures from a joint observing campaign of a limb active region between CDS and Norikura in August 1997. In this work we use the Coronal Diagnostic Spectrometer (CDS) on SOHO to determine the temperature in an active region, and the Norikura Solar Observatory (NSO) 25 cm coronagraph to measure the line widths accurately. Using these datasets we can determine the value of the V_{nt} without assuming a single temperature throughout the active region. Sect. 4 shows analysis of a CDS time series study and the correlation with the dynamics and flows of the loop structures perpendicular to the field of view. Finally conclusions are drawn and the implications for active region loop heating are discussed.

2. Observations

For the calculation of the V_{nt} at coronal temperatures we employed data from an observing campaign which took place from the 23 August – 31 August 1997 using the 25 cm coronagraph at the Norikura Solar Observatory and the CDS. CDS observed in a variety of lines enabling us to calculate the spatial distribution of temperatures. The Norikura spectrograph provides high resolution spectral imaging data in the Fe XIV 5303 Å line which provides accurate line widths. Combining CDS and Norikura observations permits the determination of V_{nt} without assuming a single fixed temperature throughout the active region.

For the determination of the dynamical behaviour of loops as a function of temperature the CDS was used. A time sequence was carried out on 17th Jan 1998, which covered lines formed over a range of temperatures from the cool transition region to the hot corona.

Details of the CDS and Norikura Coronagraph are given below.

2.1. The Coronal Diagnostic Spectrometer

Details of the CDS instrument are described by Harrison et al. (1995). CDS consists of two spectrometers – the Normal Incidence Spectrometer (NIS) and the Grazing Incidence Spectrometer (GIS). In this work we use the NIS which is stigmatic and covers the wavelength ranges: 308–381 Å and 513–633 Å. The line widths in NIS-1 and NIS-2 are both dominated by the instrumental width, so in order to obtain accurate values of V_{nt} it was necessary to combine the diagnostic capability of CDS with the higher spectral resolution of the Norikura coronagraph.

2.2. The Norikura Solar Observatory

We used the 25 cm aperture coronagraph with a high dispersion Littrow spectrograph at the Norikura Solar Observatory to measure the width of the coronal emission line Fe XIV 5303 Å. The width of the slit was 120 μm, resulting in a 3$''$ slit width. The detector is a CCD with pixel sizes corresponding to 1$''$. A 2x2 pixel on-chip summation was used along the slit resulting in a spatial sampling of 2$''$ along the slit and 3$''$ perpendicular to it. Each slit scan (3$''$) had an exposure time of 20 s, resulting in a total time of 25 mins to complete the image. A spectral resolution of 4×10^5 was used, and the spectral sampling was 0.062 Å per 54 μm, which was small enough to measure the

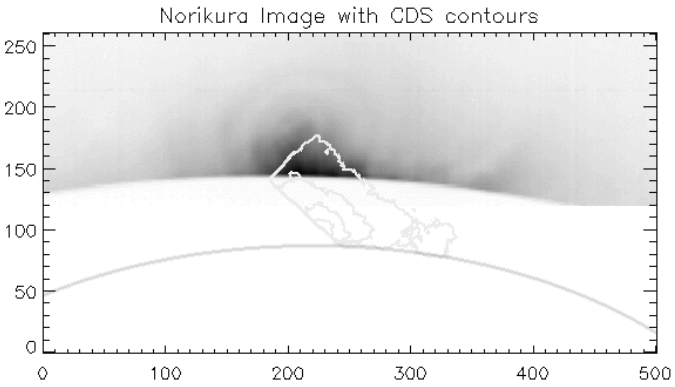

Fig. 1. Image of AR NOAA 8073 from the Norikura coronagraph on the 26 Aug 1997 23:19–23:44 UT in the coronal green line. The image is 768 × 225 arcsecs. The CDS image of Fe XIV 334 Å is shown in contours (240 × 100 arcsecs). The units are in Norikura pixels. The edge of the occulting disk and the limb of the Sun in the CDS contours are clearly seen.

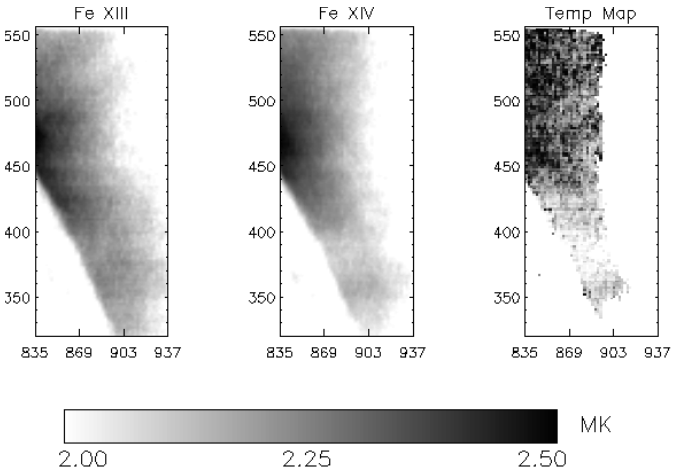

Fig. 2. CDS images of Fe XIII and Fe XIV. The images are rastered with the 4.06″ slit giving a pixel resolution of 4.06″ × 1.65″. The raster starts at 23:06 and ends at 23:54 UT. The temperature map is derived from the intensity ratio of Fe XIII and Fe XIV The CDS raster number is s8996r03. The size of the images are 102 × 240 arcsecs with the centre of the images located at -869,336 arcsecs relative to the Sun centre

emission line width of ∼ 1 Å. For the wavelength and intensity calibrations we obtained the disk-center photospheric spectrum by removing the occulting disk after the coronal observations.

3. Non-thermal velocity of coronal loops

The Norikura image is shown in Fig. 1 along with the CDS image in contours. The Norikura image is Fe XIV 5303 Å (3p $^2P_{1/2}$ – $^2P_{3/2}$), and the CDS image is Fe XIV 334 Å (3p $^2P_{1/2}$ – 3p^2 $^2D_{3/2}$). The alignment between the datasets was achieved by firstly scaling the images for the different pixel sizes. The CDS pixel size is 4.06″ × 1.65″, and the Norikura pixel size is 3″ × 2″. Then the CDS limb was placed at 0.1R$_\odot$ below the edge of the coronagraph. Then the images were automatically shifted

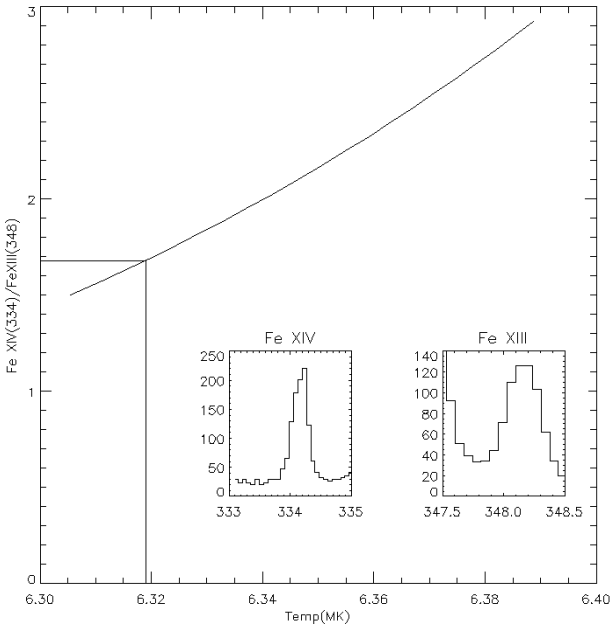

Fig. 3. The intensity ratio (Fe XIV/Fe XIII) used to determine the temperature. Sample spectra are shown – the ratio deduced from these particular lines is 1.68 giving a temperature of 2.1 MK.

until the position with the highest linear correlation coefficient was found.

The duration of the CDS raster did not exceed 50 mins. This limitation was enforced to ensure that the loop structures did not significantly change during the timescale of the observation. The temperature diagnostic used is the Fe XIV (334 Å)/Fe XIII (348 Å) intensity ratio which is described by Brosius et al. (1994). As can be seen in Fig. 2 the overall morphology of Fe XIV and Fe XIII is similar. Our derived ratio ranged between 1.6–2.9 leading to temperatures in the range T$_e$=2 – 2.45 MK. This is illustrated in Fig. 2 which shows temperature differences in the derived temperature map of up to 0.5MK. Fig. 3 shows the temperature diagnostic used with typical lines profiles of Fe XIV and Fe XIII. Both lines were fitted by standard Gauss fitting with a linear background removed. The blend to the blue side of the Fe XIII line does not significantly affect the line intensities determined. The calculated temperatures are within the temperature range of the contribution function. The electron temperatures are combined with the values of the line width determined from the Norikura coronagraph. An example of a Norikura spectral profile is shown in Fig. 4. The Norikura spectral profiles are Gaussian.

The non-thermal velocity was derived from the temperature obtained from CDS and the line widths from Norikura coronagraph shown in Figs. 3 and 4 respectively. Non-thermal velocity is defined as V$_{nt}$= $[2k(T_D - T_e)/m_i]^{1/2}$, where T_D is the Doppler temperature derived from the total observed line width, T_e is the electron temperature obtained from line ratio diagnostics and m_i is the mass of the ion considered. In all cases the total width of the lines (T_D) is larger than the thermal width as calculated from the electron temperature. A histogram

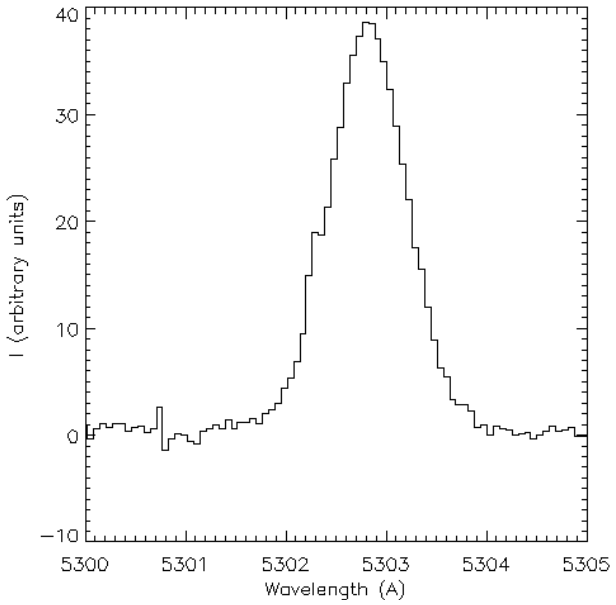

Fig. 4. An example of the Fe XIV 5303 Å line from the Norikura coronagraph. The width of the line is 0.8 Å, with the Doppler shift of -3 km s^{-1}.

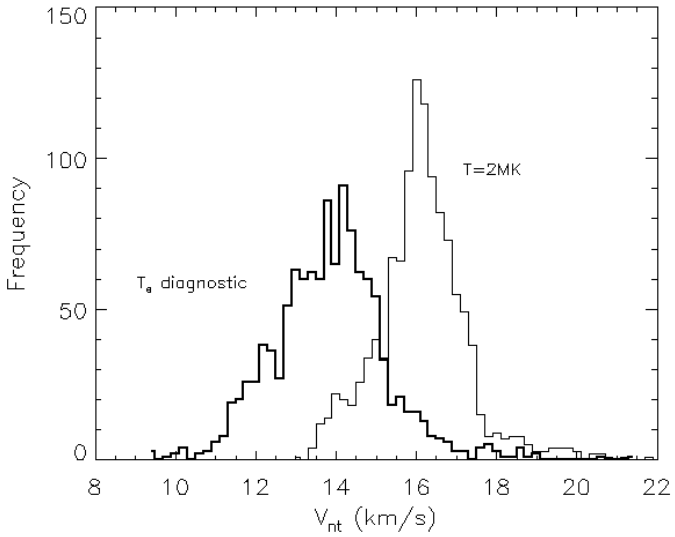

Fig. 5. Histograms of the non-thermal velocity. The thick line is calculated using the temperature diagnostic described above, and the thin line is derived by assuming a temperature of 2MK giving an average value of V_{nt}= 16.1 $\pm$ 0.8 km s^{-1}. The thick line is determined using the temperature diagnostic Fe XIV/Fe XIII giving an average value of 13.8 $\pm$ 1.2 km s^{-1}.

of the calculated non-thermal velocity is shown in Fig. 5. The V_{nt} calculated with the assumption of no variation in the temperature throughout the active region structure is higher than that determined by making use of the temperature map derived from CDS.

We assume in calculating V_{nt} that the ion temperature T_i is equal to the electron temperature T_e, and hence the excess width is due to a "non-thermal" component. Doyle et al. (1998) also assume that $T_i = T_e$ since the equilibration time is less than 1 s. In our case, for example to reach equilibrium for T_i = 2.7 MK and T_e = 2.3 MK takes only 3.7 secs (Spitzer (1956) gives equations for equilibration times). This assumes a density of 5×10^9 cm^{-3} which is derived from the Fe XIV 353/334 Å intensity ratio. Since the equilibration time is much smaller than our observing time we can assume that $T_i = T_e$, as in the case of Doyle et al. (1998). Also, the power required to maintain a temperature difference between the electrons and ions would be at least a factor of 100 greater than the radiative power loss expected - this is discussed in Bruner & McWhirter (1979) and Mariska (1992). It is also possible that static ionization equilibrium does not hold and hence the electron and ion temperatures are greater than the ionization balance. This is most likely to occur in regions with a high temperature gradient, which is not the case in quiescent coronal active region loops.

Fig. 6 illustrates the variation of the line broadening with temperature. The temperature plot shows data from previous observations alongwith our derived value. The behaviour below log T_e= 5.7 has been shown many times to increase with increasing temperature. However as temperatures above log T_e= 6 are reached, the relationship becomes less clear with a wide range of values being derived. Our averaged data shows a magnitude of V_{nt} = 13.8$\pm$1.2 km s^{-1} which is lower than previously calculated, suggesting that the V_{nt} reaches a maximum and starts to decrease as coronal temperatures are reached. The V_{nt} value decreases when the assumption that the temperature is isothermal in the radial direction is removed. This can also be seen in the V_{nt} histograms shown in Fig. 5. This is true for active regions at log $T_e\approx$ 6.4. Dmitruk et al. (1998) have carried out numercial simulations of an externally driven 2-D magnetohy-

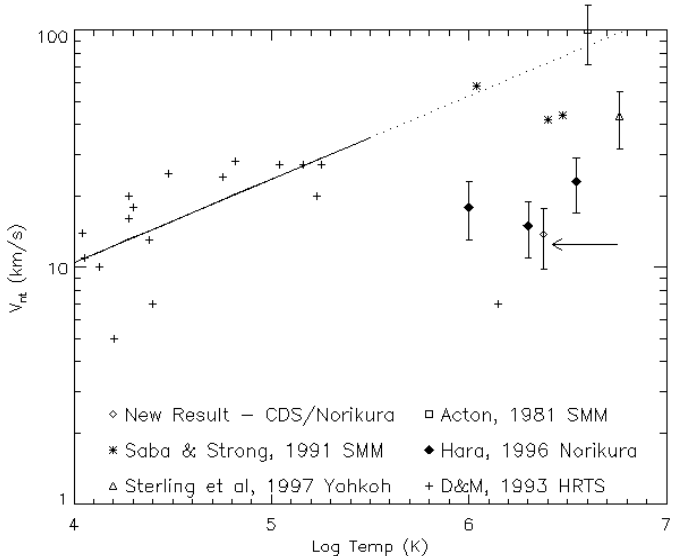

Fig. 6. This plot illustrates the variation of V_{nt} with temperature. Values of V_{nt} from previous observations are shown alongwith our new result (indicated with an arrow). The errors from this result are derived from fitting the histogram of the spread of non-thermal velocities derived over the overlapping region of the Norikura and CDS FOV (Fig. 5) and deriving the FWHM of the spread of V_{nt}.

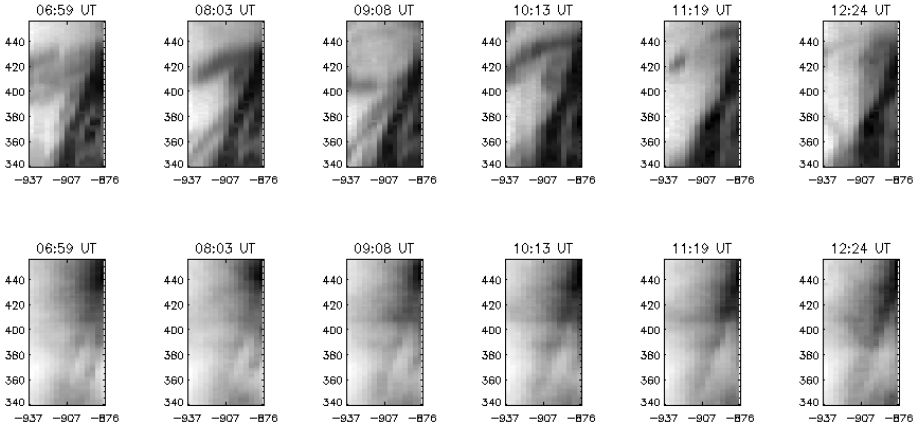

Fig. 7. A time series of images in the O V line (*top*) and Mg X line (*bottom*). The scale is in arcsecs. The OV images show frequent changes in loops brightening and disappearing. The Mg X structure remain relatively stable throughout the time series.

drodynamic (MHD) system to model the dynamics of a coronal loop. Their derived value of V_{nt} is 16 km s^{-1} which is consistent with our results. They suggest that the larger values of V_{nt} observed by Saba & Strong (1991) correspond to hotter and larger active regions. Our observations could only be carried out for log $T_e \approx$6.4. Above this temperature, it is possible that the V_{nt} values may start to increase again. A large statistical study would have to be carried out to determine whether the higher values derived at higher temperatures are due to poor (or no) spatial resolution, assumption of radial isothermality, or magnetically complex regions.

It has been well observed (e.g. Kjeldseth-Moe & Brekke 1998) that high-lying loops with temperatures below log T=5.8 are much more dynamic and unstable than loops with log T $>$ 6. This is expected since this particular class of high-lying cool loops have heights which are larger than the scale heights predicted from their temperatures. In the next section we investigate the dynamical behaviour of active region loops at different temperatures and relate this to the dependence of V_{nt} with temperature.

4. Loop dynamics

As mentioned in the introduction it is now well observed that not only do cool ($<$ 1MK) loops exist, but they are also more dynamic than their hotter counterparts. In this section we quantify how dynamic the behaviour is in each temperature regime. No previous attempt has been made to directly relate the dynamical behaviour of loops with log T_e $<$5.8 to temperature.

To achieve this, a CDS time series sequence (EPHAR_4 s10267) was carried out on the 17 Jan 1998 at a small active region on the limb in order to quantify the dynamics of the different temperature loops. Fig. 7 shows sample images in the OV and Mg X lines over a period of $\approx$ 5 hours with a cadence of $\approx$ 7 mins. As expected the OV loop shows rapid changes, whereas the Mg X loop stays relatively static.

To demonstrate the changes in the structures with time, the correlation (linear Pearson correlation coeffient, r) of each image relative to the first image observed has been calculated (Fig. 8), where x is the intensity in the x direction and y is the intensity along the slit.

Table 1.

Ion	Wavelength (Å)	Temperature (MK)
He II	584.33	0.04
O III	599.59	0.1
O V	629.73	0.22
Mg IX	368.02	0.9
Mg X	624.95	1.1
Si X	356.05	1.3
Fe XII	364.47	1.5
Si XII	520.67	1.8

$$r = \frac{\sum_i (x_i - \overline{x})(y_i - \overline{y})}{\sqrt{\sum_i (x_i - \overline{x})^2} \sqrt{\sum_i (y_i - \overline{y})^2}} \quad (1)$$

where r=1 defines a complete positive correlation and r=0 defines no correlation. The correlation decreases with time for both the hot (Mg X) and the cool (O V) loops – however the O V loop fluctuates greatly. This behaviour has been observed in many active region studies with CDS. The variability is defined as the standard deviation (σ) of the derivative of the correlation with respect to time ($\sigma(dr/dt)$). The time derivatives of the correlation for Mg X and O V are shown in Fig. 9. Fig. 10 shows the variability with temperature. This provides a measurement of how much the loop structure varies in the different temperature loops. This was calculated for the lines listed in Table 1. The Doppler velocities for the He I, O III and O V were also calculated and found to range between $\approx \pm$ 40 km s^{-1}. The values of Doppler shifts for coronal Si XII active region loops are significantly smaller with values of between 0–10 km s^{-1}. This is consistent with the analysis of Brekke et al. (1997). The variability is an indication of the dynamical behaviour perpendicular to the line of sight. These are consistent with the values of Doppler flows in that for cool loops the variability and the Doppler flows are high, and for the hot coronal loops, both the variability and Doppler flows are low.

Fig. 10 shows the variability as a function of temperature. The behaviour of the variability with temperature is similar to the behaviour of the line broadening with temperature (Fig. 6). Fig. 11 shows the variability with temperature and V_{nt} with temperature. Both relationships are linear with *variability* $\propto$

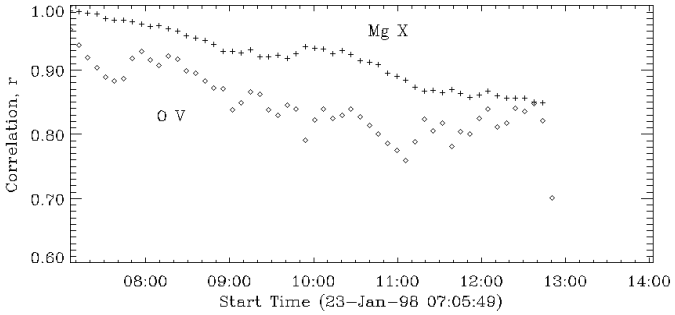

Fig. 8. The correlation, r, of each image relative to the first image in the time series for both OV and Mg X. This emphasises the changes occuring in the OV loops.

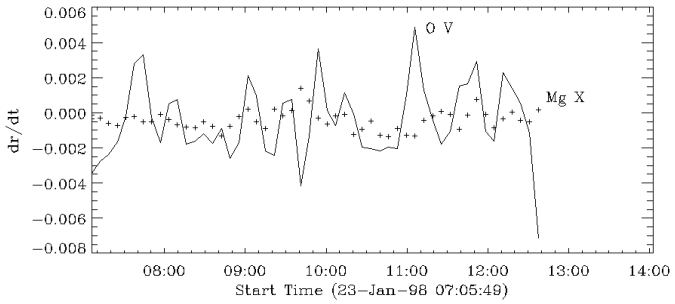

Fig. 9. The derivative of the correlation,r, with time. OV is shown as a solid line and Mg X as stars.

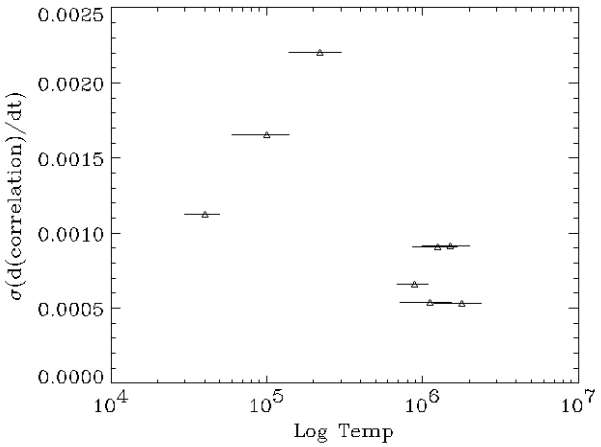

Fig. 10. The time variability ($\sigma(dr/dt)$) of the different temperature loops.

$T_e^{0.39}$ and $V_{nt} \propto T_e^{0.35}$. Since our campaign with Norikura only enabled observations of the Fe XIV emission line, and the line widths in CDS are predominantly due to instrumental width, we use the values of V_{nt} from Dere & Mason (1993) below log T_e=5.8 where the values are well established. Below log T_e=5.8, both the variability and the V_{nt} show positive gradients of approximately the same value suggesting that the line broadening is due to multi-directional flows. Consequently, the heating mechanism for the cool loops must be a transient, random mechanism, which produces flows in all directions.

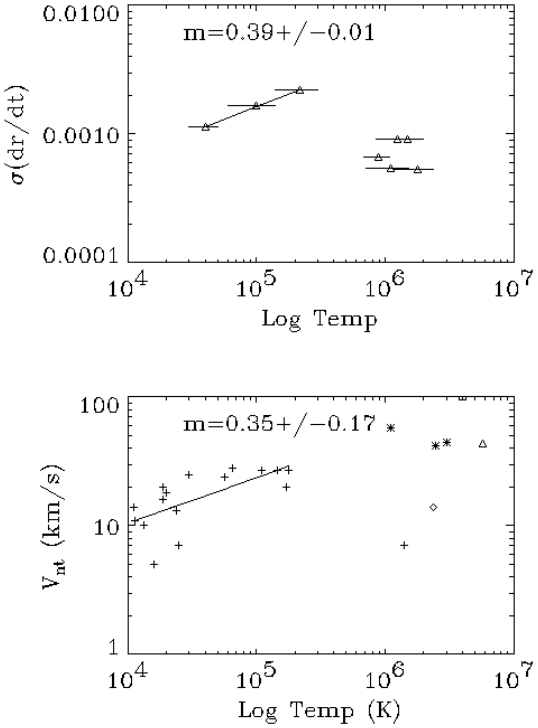

Fig. 11. The time variability ($\sigma(dr/dt)$) vs temperature (*top*), and V_{nt} vs temperature (*bottom*) (see Fig. 6 for description of data sources). The gradients of the two plots are the same within the error bars.

5. Discussion

The behaviour of line broadening in the active region corona is not well understood. Making use of the diagnostic capabilities of CDS along with the accurate line widths from the Norikura Solar Observatory, Japan, we have been able to measure the non-thermal velocities accurately without assuming that the active region is isothermal throughout the loop structures. The results indicate that there is a distinct change in the behaviour of V_{nt} with temperature as coronal temperatures are reached. As coronal values are reached the V_{nt} does not continue to increase with temperature, but decreases dramatically, which is consistent with some previous observations. The values we have derived are consistent with values determined by Dmitruk et al. (1998) using 2D MHD simulations. They also expect V_{nt} to increase with increasing temperature for coronal loops. In Fig. 6 for log T_e >6.4, there is a trend for V_{nt} to increase with increasing temperature. However, this would need to be clarified by carrying out a large statistical study over a wide range of different temperature active regions using a range of different coronal lines for analysis.

For active regions, the V_{nt} values previously determined from "transition region" temperatures cannot be assumed to be from layers in the loops, but can be considered to arise from separate entities (Matthews & Harra-Murnion (1997), Feldman (1983)). This subsequently means we cannot think of a wave travelling through an active region loop which is stratified in temperature, but we must consider each temperature loop as a

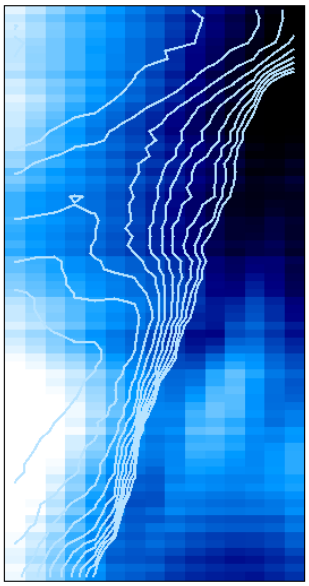

Fig. 12. Mg X image averaged over the time sequence. The contours show the O V image averaged over the time series. These ignore the intense disk emission seen in OV and concentrate on the loop structure.

separate structure. Why then are the larger values of V_{nt} observed in loops that contain lower temperature material?

It is known that for OV loops (T_e=0.2MK), large flows of order 50–100 km s^{-1} have been observed whereas measurements from FeXIV indicate small flows on the order of a few km s^{-1}. Wilhelm (1997) discovered Doppler velocities of up to 40 km s^{-1} in an active region observed in OVI and the velocity maps are indicative of the presence of whirling motions. We found that V_{nt} correlates strongly with the variability of the active region loops. This is suggestive of the excess line broadening below 1 MK being caused by multi-directional flows due to the rapidly changing structures.

There are two options to explain the dynamic cold loops. The first is that they exist as a progressive stage to the hotter loops and secondly that they are entirely separate entities. Both of these options are discussed in the following subsections in light of our results.

5.1. High-lying cool loops: a stage in the heating of coronal loops

Peres (1997) has compared various models with observations of OV loops and has shown that such loops cannot be in a steady state. The loop heights are larger than the pressure scale heights expected by a factor of approximately 5, suggesting that the loops cannot be in hydrostatic equilibrium. Peres illustrates that steady state siphon flow models cannot predict the observations of high-lying dynamic cool loops. He suggests that loops may be dynamically heated by microflares and may alternate between chromospheric and coronal conditions. Our observations support the idea of the cooler material being heated randomly and dynamically, and hence in that respect support the idea of microflare heating. Since the cool loops are showing different segments of loops brightening and fading, it may be possible that this is a route to heating the hotter coronal loops. We averaged the data over the time series available ($\approx$ 7 hrs). The averaged data for Mg X, and the contours for O V are shown in Fig. 12. We only concentrated on the loop information in OV, ignoring the bright disk emission. The averaged loop structure in OV shows similar structure to the MgX structure. This gives a qualitative indication that it is possible that the cool loops could be a stage in the heating of the hot loops.

5.2. High-lying cool loops: a separate entity

There are only a small number of cool loops at any one time relative to the large regions of higher temperature emission as can be seen from Fig. 2. This gives the impression that the cool loops are separate entities. Also, the general appearance of the cool and hot loops is dissimilar. The difference in contrast between the different temperature loops and the size scales are discussed by Matthews et al. (1999). The most obvious difference is the diffuse nature of the coronal loops whereas the cool loops have very high contrast. These observations suggest that the cool and hot loops are completely separate entities which co-exist together. Cool loops are very dynamic, not as frequent as their hot counterparts, and have high contrast. The hot loops are quasi-static at 2MK, and are very diffuse. The difference in their characteristics suggest different heating mechanisms. The highly dynamical nature of the cool loops ($<$ 1MK) is suggestive of random microflare heating.

This dynamical behaviour changes when coronal temperatures are reached, suggesting that there are different heating mechanisms in action for the different temperature regimes. Yoshida & Tsuneta (1996), suggested that plasma in the coronal loops appears to be heated by two different mechanisms in the temperature range 3–4 MK and $>$ 5MK. For example, Hara & Ichimoto (1999) searched for a dependence of V_{nt} on the loop orientation as would be expected from Alfvén waves for lower temperature coronal loops ($\approx$ 2 MK). They found a small dependence on orientation and concluded that although this may indicate that Alfvén waves contribute to the excess line width, they cannot fully explain the values of V_{nt} which are observed. Different heating mechanisms may also help to explain the wide range of values of V_{nt} which have been observed above 1MK. It has been shown that the V_{nt} for flares observed by the Yohkoh Bragg Crystal Spectrometer are independent of flare size (Harra-Murnion et al. 1997). So the small flares are also showing large values when flaring activity is occurring. Small flaring events may explain the higher values of V_{nt} which are observed for log $T_e > 6.6$.

If the cool and hot loops are separate entities we need to understand how they can coexist. Berger (1994) and references therein discuss how twisting and braiding of magnetic fields can release magnetic energy to heat coronal loops. Different levels of twist can exist - fragmentation of footpoints produces higher twist. Since the cool loops are dynamic and infrequent they may be caused by very high twisting of magnetic fields and short duration energy release which does not enable coronal temper-

atures to be reached. This is different from the understanding of the quiet Sun, where systematic downflows are observed in the middle transition region (e.g. Brekke et al. 1997). Wikstol et al. (1998) conclude from this observation that the consistent downflow cannot be reconciled with a very tangled field configuration due to the lack of randomness. However, in active region cool loops, the dynamics that we have observed along with the random high velocity flows would suggest that this is due to random events caused by a highly twisted magnetic configuration.

The Transition Region and Coronal Explorer (TRACE) will allow us to investigate the degree of field line twisting in cool loops relative to that observed in hotter loops. This would provide an opportunity to distinguish whether the cool loops are indeed different structures.

6. Conclusion

In summary we found that the value of the V_{nt} at around 2 MK ranges between 10–20 km s^{-1}. This value was determined by using temperature diagnostics rather than assuming an electron temperature. This confirms that V_{nt} does not continue to increase with temperature beyond 1MK, but decreases from 40 km s^{-1} at log T_e=5.6 to 15 km s^{-1} at log T_e=6.3. There is some evidence in other work that above log T_e=6.6 (see Fig. 6), that the V_{nt} starts to increase again with temperature.

With the recent observations from SOHO confirming the existence of cool transition region loops, we investigated the relationship that the behaviour of these loops have to the V_{nt} values. We can no longer assume that the transition region emission in active regions is a transitional layer between the surface and the hot coronal loops. We investigated one of the properties which would most likely affect the line widths - the dynamics of the different temperature loop systems. We found similar relationships between the variability and V_{nt} as a function of temperature (log T_e <5.8). This suggests that the V_{nt} is due to multiple Doppler flows which are superimposed. Above 1MK the relationship was not as clear. It is possible that since there is no relationship between the variability and V_{nt} that a different heating mechanism exists. However there were a limited number of data points to confirm this.

Acknowledgements. LKHM and SAM would like to thank PPARC for postdoctoral funding. We are grateful to the referee for improving the clarity of the paper.

References

Acton L.W., Wolfson C.S., Joki E.G., et al., 1981, ApJ 244, L137
Berger M.A., 1994, Space Sci. Rev. 68, 3–14
Boland B.C., Dyer E.P., Firth S.G., et al., 1975, MNRAS 171, 697
Brekke P, Hassler D., Wilhelm K., 1997, Solar Phys. 175, 349
Brekke P., 1998, In: Alissandrakis C., Schmieder B. (eds.) ASP conf Ser 155
Brekke P., Kjeldseth-Moe O., Harrison R.A., 1997, Solar Phys. 175, 511
Brosius J.W., Davila J.M., Thomas R.J., Thompson W.T., 1994, ApJ 425, 343
Bruner E.C., McWhirter R.W.P., 1979, ApJ 231, 557
Dere K.P., Mason H.E., 1993, Solar Phys. 144, 217
Dmitruk P., Gomez D.O., DeLuca E.E., 1998, ApJ 505, 974
Doschek G.A., Feldman U., VanHoosier M.E., Bartoe J.D.F., 1976, ApJS 31, 417
Doyle J.G., Banerjee D., Perez M.E., 1998, Solar Phys. 181, 91
Feldman U., 1983, ApJ 275, 367
Fludra A., Brekke P., Harrison R.A., et al., 1997, Solar Phys. 175, 487
Hara H., 1996, Ph.D. Thesis, National Astronomical Observatory
Hara H., Ichimoto K., 1999, ApJ, in press
Harra-Murnion L.K., Akita K, Watanabe T., 1997, ApJ 479, 464
Harrison R.A., Sawyer E.C., Carter M.K., et al., 1995, Solar Phys. 162, 233–290
Jordan C., 1991, In: Ulmschneider P., Priest E.R., Rosner R. (eds.) Mechanisms of Chromospheric and Coronal Heating. Springer-Verlag, p. 300
Kjeldseth-Moe O., Brekke P., 1998, Solar Phys., accepted
Mariska J.T., 1992, The Solar Transition Region. Cambridge Univ. Press, Cambridge
Mariska J.T., Feldman U., Doschek G.A., 1978, ApJ 226, 698
Mason H.E., Young P.R., Pike C.D. et al., 1997, Solar Phys. 170, 143
Matthews S.A., Harra-Murnion L.K., 1997, Solar Phys. 175, 541–551
Matthews S.A, Klimchuck J., Harra-Murnion L.K., 1999, A&A, submitted
Orall F.Q., 1981, A Monograph from Skylab Solar Workshop III, Colorado Associated University Press
Peres G., 1997, Fifth SOHO Workshop, ESA SP-404
Saba J.L.R, Strong K.T., 1991, ApJ 375, 789
Sheeley N.R., 1980, Solar Phys. 66, 79
Spitzer L., 1956, Physics of Fully Ionized Gases. Interscience, New York
Sterling A.C., 1997, ApJ 478, 807
Tsubaki T., 1975, Solar Phys. 43, 147
Wilhelm K., 1997, Fifth SOHO Workshop, ESA SP-404
Yoshida T., Tsuneta S., 1996, ApJ 459, 342